

# **IEICE** **TRANSACTIONS**

## **on Electronics**

**DOI:10.1587/transele.2023FUS0002**

**Publicized:2024/06/04**

**This advance publication article will be replaced by  
the finalized version after proofreading.**

**A PUBLICATION OF THE ELECTRONICS SOCIETY**



**The Institute of Electronics, Information and Communication Engineers**

**Kikai-Shinko-Kaikan Bldg., 5-8, Shibakoen 3chome, Minato-ku, TOKYO, 105-0011 JAPAN**

## BRIEF PAPER

# Electrical and X-ray Photoelectron Spectroscopy Studies of Ti/Al/Ti/Au Ohmic Contacts to AlGa<sub>0.25</sub>N/GaN

Hiroshi OKADA<sup>†a)</sup>, Member, Mao FUKINAKA<sup>†</sup>, and Yoshiki AKIRA<sup>†</sup>, Nonmembers

**SUMMARY** Effects of Al thickness in Ti/Al/Ti/Au ohmic contact on AlGa<sub>0.25</sub>N/GaN heterostructures are studied. Samples having Al thickness of 30, 90 and 120 nm in Ti/Al/Ti/Au have been investigated by electrical and X-ray photoelectron spectroscopy (XPS) depth profile analysis. It is found that thick Al samples show lower resistance and formation of Al-based alloy under the oxidized Al layer.

**key words:** AlGa<sub>0.25</sub>N/GaN heterostructure, ohmic contact, Ti/Al/Ti/Au, XPS

## 1. Introduction

Wide band gap semiconductors such as GaN and related materials are promising materials for next-generation high-efficiency power electronic devices. Particularly, AlGa<sub>0.25</sub>N/GaN heterostructures for high electron mobility transistor (HEMT) have the potential for high-speed and low sheet resistance devices due to the high mobility and high sheet carrier density two-dimensional electron gas (2DEG) at the interface. Low resistance ohmic contact formation is a crucial aspect in the fabrication of AlGa<sub>0.25</sub>N/GaN devices as parasitic resistance resulting from the contact resistance directly affects the on-resistance of HEMTs. Among the various metal combinations used for ohmic contacts in AlGa<sub>0.25</sub>N/GaN, [1] Ti/Al/Ti/Au [2] is a widely used combination. A critical parameter in determining the characteristics of these ohmic contacts is the thickness of the metal layers. Thin metal layers offer advantages of cost and productivity, however, they may come with the disadvantage of increased contact resistance due to the influence of surface oxidation on the metal electrodes. In Ti/Al/Ti/Au, the thickness of Al seems a key parameter of the contact because a sufficient amount of Al-based alloy should be formed with overcoming the Al oxidation during/after the annealing. Due to the high-temperature annealing required to achieve good ohmic contacts with the AlGa<sub>0.25</sub>N/GaN, the diffusion and intermixing (alloying) of metals and semiconductor materials are inevitable. An approach involving electrical and chemical analysis for samples with varying Al thickness is valuable for comprehending the formation of low resistance ohmic contacts. In this study, we investigate the Al thickness dependence on the Ti/Al/Ti/Au ohmic contact characteristics on AlGa<sub>0.25</sub>N/GaN. Samples having Al thickness of 30, 90, and 120 nm in Ti/Al/Ti/Au on AlGa<sub>0.25</sub>N/GaN were fabricated and

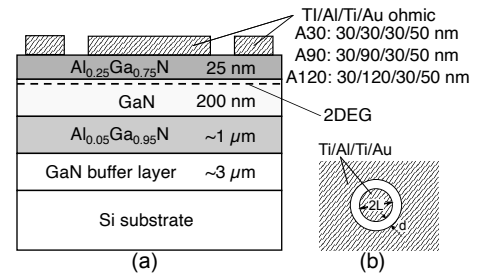


**Fig. 1** (a) Cross-section of AlGa<sub>0.25</sub>N/GaN heterostructure used in this study. Samples of A30, A90 and A120 having Al thickness of 30, 90 and 120 nm, respectively, were prepared and characterized. (b) Schematic of sample of circular transmission line model (c-TLM) structure.

characterized by electrical measurement and X-ray photoelectron spectroscopy (XPS).

## 2. Experimental

Figure 1 shows a schematic cross-section of AlGa<sub>0.25</sub>N/GaN heterostructure used in this study. AlGa<sub>0.25</sub>N/GaN heterostructure grown on Si (111) substrate grown by metal organic chemical vapor deposition (MOCVD) at NTT-AT was purchased and used. Ti/Al/Ti/Au ohmic electrode pattern was formed by the photolithography and lift-off process. Before the ohmic contact evaporation, the samples were treated with HCl:H<sub>2</sub>O=1:3 at room temperature for 2 min to remove native surface oxide followed by a rinse in deionized water. Successful evaporation of Ti, Al, Ti and Au was carried out in this order without breaking the vacuum by a multi hearth e-beam evaporation system with base pressure below  $5 \times 10^{-5}$  Pa. The evaporation thickness of each metal was monitored by a quartz crystal thickness monitor, which was calibrated by measuring the step height of the single layer by the surface stylus meter. In this study, samples of A30, A90 and A120 having Al thickness of 30, 90 and 120 nm, respectively, were prepared and characterized. All samples have been thermally annealed at 900°C for 1 min in N<sub>2</sub> ambient in a rapid thermal annealing (RTA) furnace.

For evaluation of contact resistance of the fabricated samples based on the circular transmission line model (c-TLM) [3], a series of two-terminal resistances of various spacing,  $d$ , between the ohmic electrodes were obtained from current-voltage ( $I$ - $V$ ) characteristics measured by Keithley 4200 semiconductor characterization system.

XPS depth profile analysis was performed with the PHI Quantera SXM-CI (ULVAC PHI) using a monochromatic Al

<sup>†</sup>Toyohashi University of Technology (TUT), Toyohashi 441-8580, Japan

a) E-mail: okada@las.tut.ac.jp

$K\alpha$  ( $h\nu = 1486.7$  eV) X-ray source. Focused X-ray beam of  $20\ \mu\text{m}$  diameter irradiated at the center of the ohmic contact having  $200 \times 1000\ \mu\text{m}$ . Sputtering for the depth profile analysis was performed with  $\text{Ar}^+$  at 2 kV in  $1 \times 1\ \text{mm}$  area for 90 s for each sputtering step. This sputtering condition is capable of an etching rate of 30 nm for the  $\text{SiO}_2$ . Because the sputtering rate depends on the target material, the depth may not be proportional to the sputtering time for complex metal alloy, direct interpretation of the sputtering step to the depth is difficult. In this study, we estimate only the final etching depth roughly based on the appearance of the Ga-N bonding components in XPS Ga3d spectra. Since the Ga-N bonding components in the Ga3d spectra were observed at the final etching steps, a sufficient final etching depth more than 100 nm can be roughly estimated.

### 3. Results and Discussion

$I$ - $V$  characteristics of the fabricated samples were analyzed to investigate the dependence of the contact resistance on the Al thickness. Figure 2 presents a summary of the total resistance,  $R_T$ , obtained from the  $I$ - $V$  measurements plotted against the spacing  $d$  in c-TLM samples of A30, A90 and A120. As shown in Fig.2, we observed a reduction of the total resistance for the equivalent spacing with an increase in Al thickness. Based on the c-TLM model and using the sheet resistance of the 2DEG,  $R_S = 395\ \Omega/\text{sq}$ , from the same AlGaIn/GaN wafer determined using the Van der Pauw method, we calculated specific contact resistance of  $6 \times 10^{-4}$ ,  $4 \times 10^{-4}$ ,  $1 \times 10^{-5}\ \Omega\text{cm}^2$  for A30, A90 and A120, respectively. These results demonstrate that the specific contact resistance are dependent on the Al thickness. Thinner Al contacts exhibits a disadvantage in achieving low contact resistance. This finding is consistent with the observations made by Meer *et al.*, who also noted that thicker Al layers result in smaller contact resistance.[4]

To further explore the impact of Al thickness in ohmic

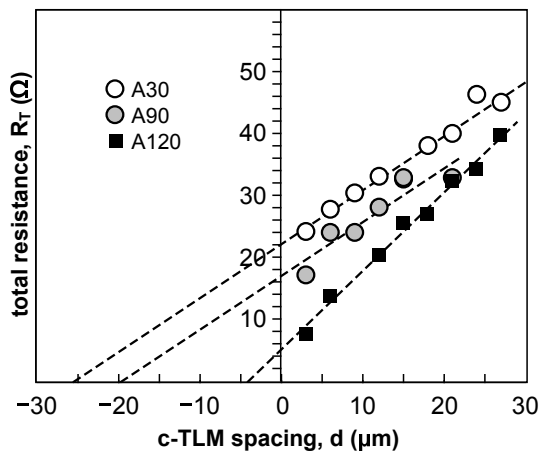


**Fig. 2** Total resistance versus spacing ( $d$ ) in c-TLM structure for sample A30, A90 and A120. Dashed lines represent fitted line using the least-square method.

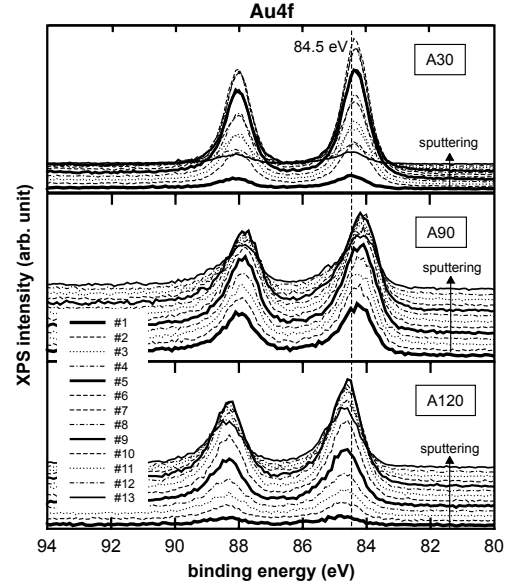


**Fig. 3** Evolution of Au4f spectra of A30, A90 and A120. Each spectrum was shifted for clarity from lower to upper following the sputtering order.

contacts, we conducted an XPS depth profile analysis. In XPS measurement, we verified the binding energy (BE) values by referring the C1s peak at 285 eV of the surface contamination layer. Figure 3 shows Au4f spectra of annealed samples confirming the reproducibility of peak energy position. For all the samples, we observed distinct peak for  $\text{Au}4f_{7/2}$  at  $84.4 \pm 0.2$  eV, accompanied by  $\text{Au}4f_{5/2}$  at around 88.1 eV. The slight shift in the peak position of  $\text{Au}4f_{7/2}$  from the BE of pure Au of 83.98 eV is attributed to the presence of Au-Al alloy[5], a phenomenon also reported in TEM observations.[6]

In Fig.4, the depth profile of metals (Ti, Al, Au, Ga) obtained from XPS peak area and the atomic sensitivity factor is presented. It is worth mentioning that the profile for A90 (not shown) resembled that of A120. Due to the thicker Al in A120, there is noticeable increase in the fraction of Al compared with A30. Interestingly, the order of the layers observed in the depth profile does not align with the sequence of evaporation. For instance the top layer of Au extends into deeper region, a phenomenon attributed to the dynamic metallurgical process during RTA. Notably, in A30,

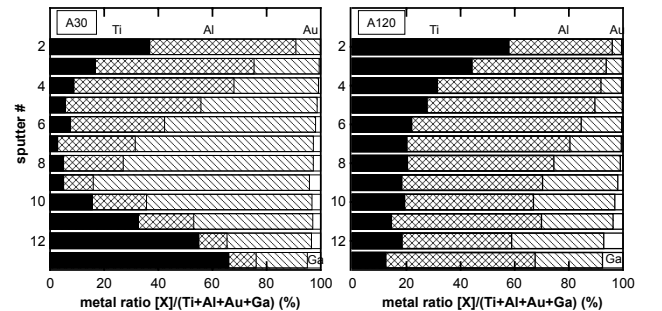


**Fig. 4** Depth profile of metals in A30 and A120.

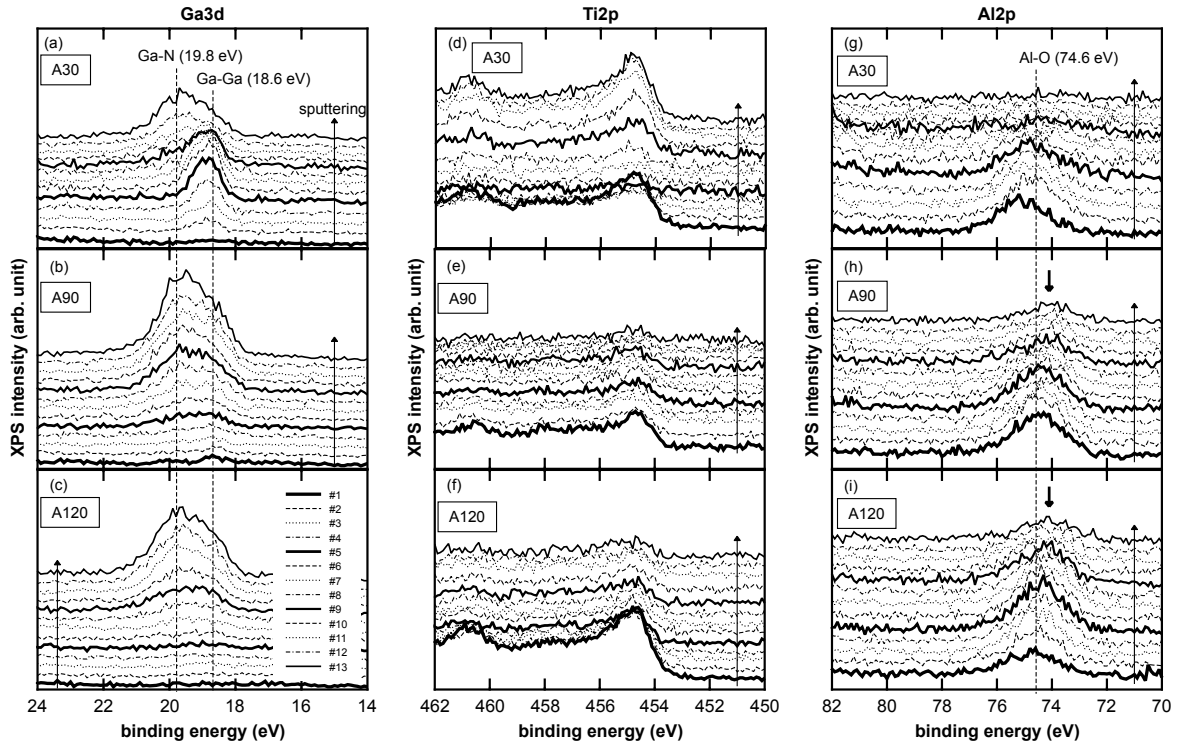


**Fig. 5** XPS spectra of Ga3d, Ti2p and Al2p of sample A30, A90 and A120. For clarity, the spectra are shifted in vertically upward direction following the sputtering order.

a distinct distribution of Ti is observed in both shallower and deeper regions. However, no such accumulation of Ti in the deeper region is observed in A120. This observation is consistent with findings in Refs.[7], [8], which suggest that Ti-GaN exhibits aggressive reactivity, while the presence of Al can mitigate this reaction. This aligns with the present profile of A120, which shows a relatively even distribution of Ti.

Figure 5 presents the evolution of XPS spectra for Ga3d, Ti2p and Al2p from samples A30, A90 and A120. For clarity, the spectra are shifted in a vertically upward direction following the sputtering order. In the case of Ga3d, all samples exhibit a distinct peak at 19.8 eV in the spectra from the deeper region, indicating Ga-N bonds. Notably, during the middle of the evolution of Ga3d peak in A30, as shown in Fig.5(a), an pronounced peak at 18.6 eV emerges. This peak is attributed to Ga metal out diffusion from AlGaN/GaN structure during the RTA process.[7], [9], [10] In Figs.5(b) and (c), Ga3d spectra of A90 and 120, respectively, also suggest the presence of Ga metal in deeper region, as indicated by the broadened signal. However, the signal attributed to Ga metal components is less pronounced compared with the A30 in Fig.5(a).

In Figs.5(d), (e), and (f), the spectra of Ti2p exhibit a similar feature with peak around 455 eV, as well as its spin splitting peak at around 463 eV. These peaks are characterized by their broad nature and higher BE side tail. It is apparent that these spectra consist of multiple components, including Ti-N at BE of 456 eV, Ti-O at 458 eV[7] together

with TiAlN at 455 eV[11]. These components appear consistently across all samples, regardless of the Al thickness.

In Figs.5(g), (h) and (i), the spectra of Al2p close to the surface showed a peak at 74.6 eV for all the samples, suggesting the presence of Al oxidation in the form of  $\text{AlO}_x$ . [9], [12]. Particularly, the Al2p peak in A30 remained at the same BE, while the peak from the deeper region almost disappeared in the spectra near sputter #9. This is consistent with the higher resistance in A30, where the Al oxide is the dominant phase in the contact. On the other hand, thicker Al samples exhibited a departure from the BE peak at 74.6 eV towards lower BE values in the deeper region, as indicated by the arrow in Fig.5(h). This behavior is more pronounced in A120, as shown in Fig.5(i). For the thick Al samples, Al alloys are thought to be formed in the deeper region, where the influence of surface oxidation is less pronounced. Garbe *et al.*[13] reported that the formation of the metallic  $\text{Al}_3\text{Ti}$  alloy in annealed Al/TiN on GaN with thick Al, as observed in their TEM and XPS characterization with appearance of BE peak at 72.4 eV, which is 2 eV lower than that of Al nitride/oxide at 74.5 eV. TiAl alloy formation is also reported in TEM observation.[14] However, in the present study, the BE shift of 0.5 eV from the Al oxide peak position in A90 and A120 cannot be explained by the formation of  $\text{Al}_3\text{Ti}$ . A plausible explanation for observed BE shift in A90 and A120 is the formation of TiAlN. Greczynski *et al.*[15] have reported that  $\text{Ti}_{1-x}\text{Al}_x\text{N}$  BE varies slightly from 74.1 with  $x = 0.25$  to 74.4 eV with  $x = 0.83$ . Chawla *et al.*[16] have described that  $\text{Ti}_{1-x}\text{Al}_x\text{N}$  exhibits lower resistivity for the

film with  $x < 0.83$  due to the insulating nature of AlN. Further detailed studies are needed for the exact identification of the Al alloy under the oxidized surface, however, the formation of observed Al alloy in thick Al samples A90 and A120 plays an important role in reducing the contact resistance. The present results indicate that Ti/Al/Ti/Au ohmic contacts with thin Al have a disadvantage for achieving low contact resistance, and the situation improves with an increase in Al thickness.

### Acknowledgments

This work was carried out using facilities of Venture Business Laboratory (VBL), Electronics-Inspired Interdisciplinary Research Institute (EIIRIS), and Cooperative Research Facility Center (CRFC) in Toyohashi University of Technology. This work was supported by JSPS KAKENHI Grant Number 20K04579, Suzuki foundation, Nitto foundation and Naito foundation.

### References

- [1] G. Greco, F. Iucolano, F. Roccaforte, "Ohmic contacts to gallium nitride materials", *Appl. Surf. Sci.*, vol. 383, pp. 324–345, 2016.
- [2] J. Hilsenbeck, W. Rieger, E. Nebauer, W. John, G. Tränkle, J. Würfl, A. Ramakrishnan and H. Obloh, "AlGaIn/GaN HFETs with new ohmic and Schottky contacts for thermal stability up to 400°C", *Phys. Stat. Sol. (a)* vol. 176, pp.183–187, 1999.
- [3] D. K. Schroder, *Semiconductor Material and Device Characterization*, pp.150-157, John Wiley & Sons, New Jersey, 2006.
- [4] M. Meer, A. Rawat, K. Takhar, S. Ganguly, and D. Saha, "Interface dynamics in ohmic contact optimization on AlGaIn/GaN heterostructure by the formation of TiN", *Microelectronic Eng.*, vol. 219, 111144, 2020.
- [5] H. Piao, M. S. Fuller, D. Miller, and N. S. McIntyre, "A study of thin film Au-Al alloy oxidation in ambient air by X-ray photoelectron spectroscopy (XPS), X-ray absorption near edge structure (XANES), and secondary ion mass spectroscopy (SIMS)", *Appl. Surf. Sci.*, vol. 187, pp.266–274, 2002.
- [6] A. N. Bright, P. J. Thomas, M. Weyland, D. M. Tricker, C. J. Humphreys and R. Davies, "Correlation of contact resistance with microstructure for Au/Ni/Al/Ti/AlGaIn/GaN ohmic contacts using transmission electron microscopy", *J. Appl. Phys.*, vol. 89, pp.3143–3150, 2001.
- [7] M. Nozaki, J. Ito, R. Asahara, S. Nakazawa, M. Ishida, T. Ueda, A. Yoshigoe, T. Hosoi, T. Shimura, H. Watanabe, "Synchrotron radiation X-ray photoelectron spectroscopy of Ti/Al ohmic contacts to n-type GaN: Key role of Al capping layers in interface scavenging reactions", *Appl. Phys. Express*, vol. 9, 105801, 2016.
- [8] B. Van Daele, G. Van Tendeloo, W. Ruythooren, J. Derluyntj, M. R. Leys, and M. Germain, *Appl. Phys. Lett.*, vol. 87, p.061905, 2005.
- [9] A. Akkaya, and E. Ayyıldız, "Depth profile study on Ti/Al bilayer Ohmic contacts to AlGaIn/GaN", *Materials Today: Proc.*, vol.46, pp.6939–6946, 2021.
- [10] M. Piazza, C. Dua, M. Oualli, E. Morvan, D. Carisetti, F. Wyczisk, "Degradation of TiAlNiAu as Ohmic contact metal for GaN HEMTs", *Microelectron. Reliab.*, vol. 49, pp.1222–1225, 2009.
- [11] A. Rizzo, L. Mirengi, M. Massaro, U. Galietti, L. Capodieci, R. Terzi, L. Tapfer, and D. Valerini, "Improved properties of TiAlN coatings through the multilayer structure", *Surf. Coat. Technol.*, vol. 235, pp.475–483, 2013.
- [12] S. Kaciulis, L. Pandolfi, S. Viticoli, M. Peroni, A. Passaseo, "Characterization of ohmic contacts on GaN/AlGaIn heterostructures", *Appl. Surf. Sci.*, vol. 253, pp.1055-1064, 2006.
- [13] V. Garbe, J. Weise, M. Motylenko, W. Münchgesang, A. Schmid, D. Rafaja, B. Abendroth, and D. C. Meyer, "Au-free ohmic Ti/Al/TiN contacts to UID n-GaN fabricated by sputter deposition", *J. Appl. Phys.*, vol. 121, 065703, 2017.
- [14] G. Greco, F. Giannazzo, F. Iucolano, R. L. Nigro, and F. Roccaforte, "Nanoscale structural and electrical evolution of Ta- and Ti-based contacts on AlGaIn/GaN heterostructures", *J. Appl. Phys.*, vol. 114, 083717, 2013.
- [15] G. Greczynski, L. Hultman, and M. Odén, "X-ray photoelectron spectroscopy studies of  $Ti_{1-x}Al_xN$  ( $0 \leq x \leq 0.83$ ) high-temperature oxidation: The crucial role of Al concentration", *Surf. Coat. Technol.*, vol. 374, pp.923–934, 2019.
- [16] V. Chawla, R. Chandra, R. Jayaganthan, "Effect of phase transformation on structural, electrical and hydrophobic properties of nanocomposite  $Ti_{1-x}Al_xN$  films", *J. Alloys Compd.*, vol. 507, pp.L47–L53, 2010.